

The NRL Layered Global Ocean Model (NLOM) with an Embedded Mixed Layer Submodel: Formulation and Tuning*

ALAN J. WALLCRAFT, A. BIROL KARA, HARLEY E. HURLBURT AND PETER A. ROCHFORD⁺

Naval Research Laboratory, Stennis Space Center, Mississippi

(Manuscript received 18 October 2001, in final form 16 April 2003)

ABSTRACT

A bulk-type (modified Kraus–Turner) mixed layer model that is embedded within the Naval Research Laboratory (NRL) Layered Ocean Model (NLOM) is introduced. It is an independent submodel loosely coupled to NLOM’s dynamical core, requiring only near-surface currents, the temperature just below the mixed layer, and an estimate of the stable mixed layer depth. Coupling is achieved by explicitly distributing atmospheric forcing across the mixed layer (which can span multiple dynamic layers), and by making the heat flux and thermal expansion of seawater dependent upon the mixed layer model’s sea surface temperature (SST). An advantage of this approach is that the relative independence of the dynamical solution from the mixed layer allows the initial state for simulations with the mixed layer to be defined from existing near-global model simulations spun up from rest without a mixed layer (requiring many hundreds of model years). The goal is to use the mixed layer model in near-global multidecadal simulations with realistic 6-hourly atmospheric forcing from operational weather center archives. A minimum requirement therefore is that there be no drift in yearly average SST over time. The dynamical layer densities are relaxed to climatology as a standard part of the NLOM model design, and this ensures that the temperature just below the mixed layer provided to the mixed layer submodel does not drift. The density relaxation below the mixed layer does not significantly dampen anomalies even on interannual timescales because the anomalies are largely defined by layer thickness variations. When combined with calculating the latent and sensible heat flux using model SST, this is sufficient to keep SST on track without any explicit relaxation to the SST climatology.

The sensitivity of the global ocean model to the choice of free Kraus–Turner parameters in the bulk mixed layer model is investigated by undertaking a tuning exercise to find a single set of parameters that provides a realistic SST from realistic atmospheric forcing over as much of the global ocean as possible. This is done by comparing the monthly Comprehensive Ocean Atmosphere Data Set (COADS) SST climatology to monthly averages from the model using a set of statistical metrics. A single set of mixed layer parameters is reported that gives excellent agreement with the SST climatology over most of the global ocean. The actual parameter values are probably specific to this coupled system, but the same methodology can be used to tune any mixed layer model with free parameters.

1. Introduction

The mixed layer of ocean general circulation models (OGCMs) plays an important role in the exchange of heat energy between the ocean and atmosphere and in

determining the upper-ocean characteristics (e.g., Gent and Cane 1989; Yuen et al. 1992; Murtugudde et al. 1995; Schopf and Loughe 1995; Hu and Chao 1999). A major challenge for mixed layer models is being able to simulate the annual mean and seasonal cycle of SST and mixed layer depth (MLD) globally in an environment of many competing processes that may not be accurately known, including air–sea exchange, oceanic transport, and vertical mixing.

Here a strong motivation is eddy-resolving global ocean prediction. In addition to SST and MLD, the impact of the mixed layer on sea surface height (SSH) is of interest because SSH is observed by satellite altim-

* Naval Research Laboratory Contribution Number JA/7320/01/0023.

⁺ Current affiliation: Spectral Sciences Incorporated, Burlington Massachusetts.

Corresponding author address: Alan J. Wallcraft, Naval Research Laboratory, Code 7323, Stennis Space Center, MS 39529-5004.
E-mail: wallcraft@nrlssc.navy.mil

etry and is a key data type for assimilation by an eddy-resolving ocean model. The first eddy-resolving global ocean nowcast/forecast system has been running in real time since 18 October 2000 and became an operational product of the U.S. Navy on 27 September 2001 (Rhodes et al. 2002; Smedstad et al. 2003). Real-time and archived results can be seen on the Web (http://www.ocean.nrlssc.navy.mil/global_nlom).

In this paper we discuss the formulation and tuning of the mixed layer embedment used in the operational prediction model. Although the operational model uses $1/16^\circ$ resolution, $1/2^\circ$ resolution is used here. The operational model has low vertical resolution (six Lagrangian dynamical layers plus the mixed layer) to make operation feasible using available supercomputer resources. Hence, key challenges were developing a mixed layer embedment that would 1) perform reliably with accurate results globally in a model with low vertical resolution and 2) do that with limited computational overhead. An adequate capability for this purpose did not already exist. In this paper, we discuss a mixed layer embedment that meets these requirements.

There are a variety of mixed layer models that can be implemented within an OGCM. Following Kantha and Clayson (1994) the vast majority of mixed layer models can be grouped under two major categories: (i) bulk mixed layer models (e.g., Niiler and Kraus 1977; Price et al. 1986), and (ii) diffusion-based mixed layer models (e.g., Mellor and Yamada 1982; Martin 1985; Large et al. 1994). There are also mixed layer models based on higher moments of the governing equations (e.g., Warn-Varnas and Piascek 1979; Rodi 1987) that include very complex parameterizations of turbulence. These are less popular because of their greater computational expense.

For the bulk-type models, the momentum and heat balance of the entire mixed layer are considered. In this type of model the deepening–shallowing of the mixed layer is determined directly using surface fluxes of momentum and buoyancy (e.g., Niiler and Kraus 1977; Garwood 1977). There are also modified versions of the classical bulk models as in Price et al. (1986). These types of models are based on shear instability by considering a Richardson number criterion. A major advantage of bulk models is their simplicity and ease of implementation because they are only weakly dependent upon the vertical resolution of the OGCM. Their major disadvantage is the need for appropriate tuning of the entrainment coefficient and an appropriate value for the bulk Richardson number when used.

Diffusion-based models focus on turbulent mixing and diffusion in the mixed layer using empirical formulations that are based on observational and theoretical surface layer information or flux-profile relationships (e.g. Stull 1988). In this type of model the deepening–shallowing of the mixed layer is due to convection and stabilizing surface buoyancy fluxes. Their major advantage is generally better performance than

bulk models. Their major disadvantage is the need for high vertical resolution of the upper ocean in order to perform well. For a more complete review of these mixed layer models the reader is referred to Kantha and Clayson (1994) and Large et al. (1994).

The evolution of the Naval Research Laboratory (NRL) Layered Ocean Model (NLOM) is discussed in Hurlburt and Thompson (1980), Wallcraft et al. (1991), Wallcraft and Moore (1997), and Moore and Wallcraft (1998). In this paper we introduce a new embedding of a bulk mixed layer model in the thermodynamic version of NLOM. It has a convective option that allows additional entrainment below the mixed layer that is not included in typical implementations of bulk mixed layer models in OGCMs. Section 2 gives the details of the mixed layer model and its embedding in the NLOM. Section 3 presents the tuning of the mixed layer model parameters, the statistical measures used to assess their influence, and the NLOM simulations performed. Finally, section 4 gives the conclusions of this study.

2. Model description

The NLOM uses a primitive equation layered formulation where the equations have been vertically integrated through each Lagrangian layer. Prognostic variables are layer density, layer thickness, and layer volume transport per unit width (layer velocity times layer thickness). The bottom topography is confined to the lowest layer and a finite layer thickness is maintained by mixing across layer interfaces. The NLOM has typically been run without an explicit mixed layer, which is equivalent to assuming that the mixed layer is always inside the upper layer (see appendix A for a detailed description of NLOM in this mode). It includes support for passive tracers and this has now been extended with an “almost passive” embedded well-mixed surface turbulent boundary layer. The version presented here builds upon an earlier implementation for the Indian Ocean (Rochford et al. 2000). It has been extended to the global ocean with significant modifications to accommodate the wider diversity of conditions, such as updated mixed layer parameterizations, use of a floating mixed layer, a new advection scheme, a modified Kraus–Turner model, and improved model temperature profile and forcing fields. A schematic illustration of the global NLOM with an embedded mixed layer is shown in Fig. 1.

One of the major advantages of NLOM over other types of OGCMs such as z -level and sigma-coordinate models is its lower computational cost for the same model domain and horizontal resolution. One reason is that we can use lower vertical resolution to realistically represent the ocean circulation. For example, in the $1/2^\circ$ model there are only seven layers in the vertical, including the mixed layer. NLOM is also a single efficient portable and scalable computer code that can run any of the model configurations on a variety of computing platforms (Wallcraft and Moore 1997). As a consequence, a 5-yr simulation

using NLOM with an embedded mixed layer takes approximately 7 h of wall-clock time on 32 Cray T3E processors. The mixed layer can reach statistical energy equilibrium in just 2–3 yr. This allows an extensive set of climatologically forced sensitivity experiments to be performed with a global OGCM that would otherwise be computationally infeasible.

a. NLOM mixed layer formulation

The surface turbulent boundary layer that is embedded within NLOM is assumed to be “well mixed.” The temperature T_m is therefore defined to be constant throughout a layer of thickness h_m and to be equivalent to the SST. The layer thickness h_m is defined as the lower bound of the turbulent boundary layer and is hence the MLD. The embedded mixed layer carries prognostic equations for SST and MLD as follows:

SST,

$$\begin{aligned} \frac{\partial T_m}{\partial t} + \mathbf{v}_1 \cdot \nabla T_m &= -\frac{\max(0, \omega_m)}{h_m} (T_m - \Delta T_m - T_b) \\ &+ \frac{Q_a - Q_p e^{-h_m/h_p}}{\rho_0 C_{pa} h_m} + \frac{K_H}{h_m} \nabla \cdot (h_m \nabla T_m); \end{aligned} \quad (1)$$

MLD,

$$\frac{\partial(h_m)}{\partial t} + \nabla \cdot (h_m \mathbf{v}_1) = \omega_m. \quad (2)$$

The reader is referred to appendix B for a description of all symbols used in the mixed layer model equations.

Major free parameters in Eqs. (1) and (2) are net surface heat flux (Q_a), temperature difference at the base of the mixed layer [$\Delta T_b = (T_m - \Delta T_m) - T_b$], and the entrainment velocity (ω_m). These free parameters are obtained, respectively, from the surface energy budget (section 2b), a continuous model temperature profile (section 2c), and a modified Kraus–Turner (KT) model (section 2d). We note here that in model simulations the Laplacian temperature diffusion in Eq. (1) is typically turned off (i.e., $K_H = 0$) because the van Leer monotonic scheme (Carpenter et al. 1990; Lin et al. 1994) employed for the advection of SST and MLD contributes sufficient nonlinear diffusion to maintain stability. The van Leer scheme also results in much sharper SST and MLD fronts, and allows the NLOM to be run using a very small minimum imposed MLD (typically 10 m). Using a range of values between 5 and 50 m we found that climatologically forced simulations are not very sensitive to a minimum MLD of less than 20 m.

The mixed layer is not confined to be within the upper dynamical layer as in earlier approaches (Rochford et al. 2000; McCreary et al. 1993). The mixed layer is allowed to penetrate to a depth greater than the thickness

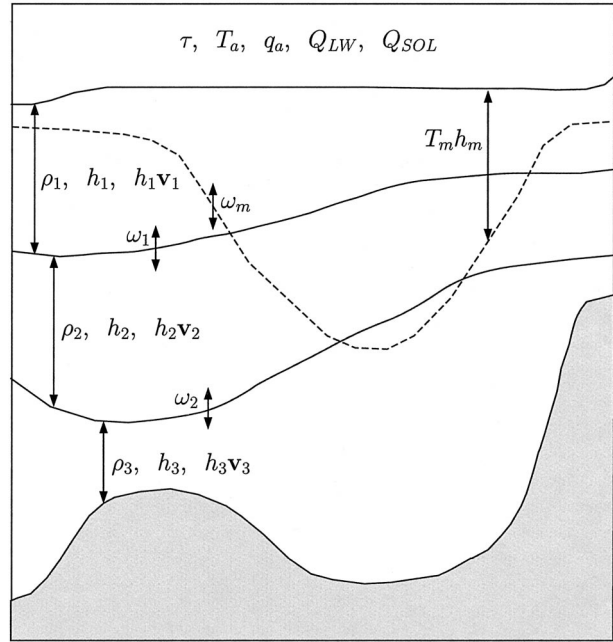


FIG. 1. Schematic illustration of mixed layer structure in the NLOM. For simplicity, only three thermodynamic layers and the mixed layer are shown although six layers plus the mixed layer are used in this study. Prognostic variables are layer density (ρ_i), layer thickness (h_i), layer transport per unit width ($h_i \mathbf{v}_i$), mixed layer temperature (T_m), and MLD (h_m). Note that mixed layer temperature (T_m) is considered to be the same as SST and that the mixed layer velocity is taken to be the layer 1 velocity (\mathbf{v}_1). Atmospheric forcing is wind stress (τ), air temperature (T_a), mixing ratio at 10 m above the sea surface (q_a), longwave radiation (Q_{LW}), and downward solar irradiance at the sea surface (Q_{SOL}).

of the first (uppermost) dynamical layer, that is, to “float” within the OGCM. While the mixed layer is to some extent independent of the dynamical layers it is not entirely passive. In particular, 1) a deep mixed layer distributes surface forcing across the multiple dynamical layers, 2) thermal expansion is based on the mixed layer temperature (T_m) rather than layer 1 temperature (T_1), and 3) surface heat flux depends on T_m . All three factors can change the steric sea surface height anomaly. However, only a redistribution of the wind stress is likely to significantly change the ocean circulation that would be simulated without the presence of a mixed layer. This allows us to spin up the model from rest to statistical equilibrium without a mixed layer (a process that takes hundreds of model years), and then run for a relatively short time (e.g., 3–5 yr) with the mixed layer.

Layer 1 velocity is used in these prognostic equations because the depth of the mixed layer under general conditions lies between the layer interfaces and is often much shallower than the first layer. Constructing a suitable vertically averaged velocity of the mixed layer from the information of the other layers is difficult given the absence of a suitable velocity profile that could be assumed a priori to exist within the layers. Given that surface currents typically dominate in the upper ocean,

and that the emphasis is on SST prediction, we simply use layer 1 velocity for the SST and MLD equations.

b. Surface energy balance

The net surface heat flux absorbed (or lost) by the upper ocean to depth z [$Q(z)$] is parameterized as the sum of the downward surface solar irradiance (Q_{SOL}), upward longwave radiation (Q_{LW}), and downward latent and sensible heat fluxes (Q_L and Q_S , respectively). The surface solar irradiance is decomposed into its infrared (IR) and photosynthetically available radiation (PAR) components as $Q_{\text{SOL}} = Q_{\text{IR}} + Q_p(0)$, respectively. The net surface heat flux is therefore written as

$$Q_a = Q_{\text{IR}} + Q_p(0) - Q_{\text{LW}} + Q_L + Q_S. \quad (3)$$

The IR and PAR components at the ocean surface ($z = 0$) can be expressed as fractions of the net solar irradiance:

$$Q_{\text{IR}} = (1 - \lambda_p)Q_{\text{SOL}}, \quad (4)$$

$$Q_p(0) = \lambda_p Q_{\text{SOL}}, \quad (5)$$

with λ_p (in general) having a dependence on space and time. Given the Q_{IR} component is absorbed within the first few centimeters, which is much less than the minimum MLD imposed in most OGCMs (10 m for NLOM), all of the IR solar irradiance arriving at the air–sea interface is considered to be absorbed by the mixed layer. A value of $\lambda_p = 0.49$ is chosen as a good approximation over most of the global ocean (Rochford et al. 2001).

Using these relations along with that for exponential attenuation of PAR (Simpson and Dickey 1981), the heat flux absorbed by the upper ocean by depth z is given by

$$Q(z) = Q_a - Q_p(z), \quad (6)$$

$$Q_a = Q_{\text{SOL}} - Q_{\text{LW}} + Q_L + Q_S, \quad (7)$$

$$Q_p(z) = \lambda_p Q_{\text{SOL}} \exp(-k_{\text{PAR}}z). \quad (8)$$

Here Q_a is the net heat flux at the ocean surface and k_{PAR} the attenuation coefficient for PAR in seawater (m^{-1}). The rate of surface heating/cooling of the mixed layer is simply obtained by evaluating this expression at the MLD (i.e., $z = h_m$). The remaining solar radiation [i.e., $Q_a - Q(h_m)$] is applied below the mixed layer. In other words, the total radiation flux in the mixed layer becomes $Q_{\text{SOL}} - Q_{\text{LW}} - Q_p \exp(-h_m/10)$, where the reference depth is taken as 10 m in the model. The total radiation flux is still $Q_{\text{SOL}} - Q_{\text{LW}}$, so the total water column needs to receive $Q_{\text{SOL}} - Q_{\text{LW}}$, which is $Q_p \exp(-h_m/10)$ more than the mixed layer. The NLOM is designed to read in k_{PAR} fields to allow for space- and time-varying attenuation of PAR, and a monthly mean dataset constructed from 1997–98 remotely sensed observations (McClain et al. 1998) from the Sea-viewing Wide Field-of-view Sensor (SeaWiFS) is currently used (Rochford et al. 2001). In the model, latent and sensible

heat fluxes at the air–sea interface are calculated using efficient and computationally inexpensive bulk formulas that include the effects of dynamic stability (Kara et al. 2002a).

In general, the model reads in the following time-varying atmospheric forcing fields: wind stress, air temperature, air mixing ratio, and net solar radiation. These are typically obtained from climatology or from archived operational weather center products. The sensible and latent heat fluxes are strongly dependent on SST and are calculated every time step using the model SST. Radiation fluxes also depend to some extent on SST but these are specified because they strongly depend on cloudiness, which is less readily available. Basing fluxes on model SST automatically provides a physically realistic tendency toward the “correct” SST. If the model SST is too high (low), the flux is reduced (increased) relative to that from the correct SST. The trend toward reality is typically not sufficient on its own to keep the model SST on track, but it is sufficient if we also have an “accurate enough” characterization of the temperature just below the mixed layer. In addition to applying the heat flux, the temperature below the mixed layer is kept on track in NLOM by relaxing the dynamic layer densities back toward climatology (monthly means interpolated to daily values in layer 1, annual otherwise). There is no direct relaxation term in the SST equation but entrainment at the base of the mixed layer allows the dynamical layer density relaxation to influence SST. The density relaxation does not significantly damp anomalies even over interannual timescales because most of the information about the anomalies is carried in the layer thickness variations. For example, NLOM maintained an El Niño–generated Rossby wave for more than a decade (Jacobs et al. 1994).

c. NLOM temperature profile

The equations of state typically used by ocean models are not simple and their computation represents an appreciable fraction of the OGCM execution time. To increase computational efficiency at a modest expense to accuracy, NLOM includes density (ρ_k) as the only thermodynamic prognostic variable for its dynamical layers and infers a layer temperature (T_k) from the density. Its equation of state is expressed as a perturbation about climatology where the climatological layer density ($\tilde{\rho}_k$) and layer temperature (\hat{T}_k) are vertical averages of the Levitus and Boyer (1994) annual climatology obtained using annual mean NLOM layer thicknesses. All of the change in density is assumed to be due to temperature as follows:

$$\rho_k(T, S) = \tilde{\rho}_k - \tilde{\rho}_k \alpha(\hat{T}_k)(T - \hat{T}_k), \quad (9)$$

$$\alpha(T) = 5.3 \times 10^{-5} + 1.2 \times 10^{-5}T - 9.7 \times 10^{-8}T^2. \quad (10)$$

The coefficient of thermal expansion at a given temperature (α) is formulated using data given in Gill (1982) for surface water at a salinity of 35 psu. We found a quadratic fit [Eq. (10)] is sufficient for all temperatures between -2° and 31°C . The dynamic layer equations maintain a minimum density contrast ($\Delta\rho_k$) between each pair of layers. Therefore, in regions of low stratification the model's own climatology ($\tilde{\rho}_k$) can be significantly different from the observed climatology ($\hat{\rho}_k$) it is relaxing toward. So for accuracy the equation of state is a perturbation about the model's own climatology. The layer temperature (T_k) is given by

$$T_k = \hat{T}_k - \frac{\rho_k - \tilde{\rho}_k}{\tilde{\rho}_k \alpha(\hat{T}_k)}. \quad (11)$$

Thus, T_k is at the observed climatology (\hat{T}_k) when the layer density is at its time-averaged value (model climatology, $\tilde{\rho}_k$), with all variation in density assumed to be from temperature. These are temperatures vertically averaged over each layer except the surface mixed layer. To provide a better representation of the temperature below the mixed layer we use a continuous profile \tilde{T} (see Fig. 2) derived from $T_m, T_k, h_k (k = 1, 2, \dots, n)$:

$$\tilde{T}(z) = \tilde{T}_k \left(z - \sum_{l=1}^{k-1} h_l \right), \quad \sum_{l=1}^{k-1} h_l \leq z < \sum_{l=1}^k h_l. \quad (12)$$

In layer n , for $0 \leq z \leq h_n$,

$$\tilde{T}_n(z) = T_n. \quad (13)$$

In layer k , for k in $n-1 \dots 2$ and $0 \leq z \leq h_k$,

$$\hat{T}_k(0) = \frac{h_{k-1}T_k + h_kT_{k-1}}{h_{k-1} + h_k}, \quad (14)$$

$$\tilde{T}_k(z) = \frac{(h_k - z)\tilde{T}_k(0) + z\tilde{T}_{k+1}(0)}{h_k}. \quad (15)$$

In layer 1, for $0 \leq z \leq z_0$,

$$z_0 = h_1 \frac{T_1 - \tilde{T}_2(0)}{\tilde{T}_1(0) - \tilde{T}_2(0)}, \quad (16)$$

$$\tilde{T}_1(0) = \max(T_m, T_1 + \Delta T_m), \quad (17)$$

$$\tilde{T}_1(z) = \frac{(z_0 - z)\tilde{T}_1(0) + zT_1}{z_0}. \quad (18)$$

In layer 1, for $z_0 \leq z \leq h_1$,

$$\tilde{T}_1(z) = \frac{(h_1 - z)T_1 + (z - z_0)\tilde{T}_2(0)}{h_1 - z_0}. \quad (19)$$

The continuous profile (\tilde{T}) is defined everywhere but only valid below the mixed layer [see Eq. (22) for the full profile]. Each layer has a linear profile from its top to bottom interface except for the top layer. The lowest interface is set to T_n so that the lowest layer's profile is constant. All other interface values are a sum of the two adjacent layer temperatures weighted by layer thickness.

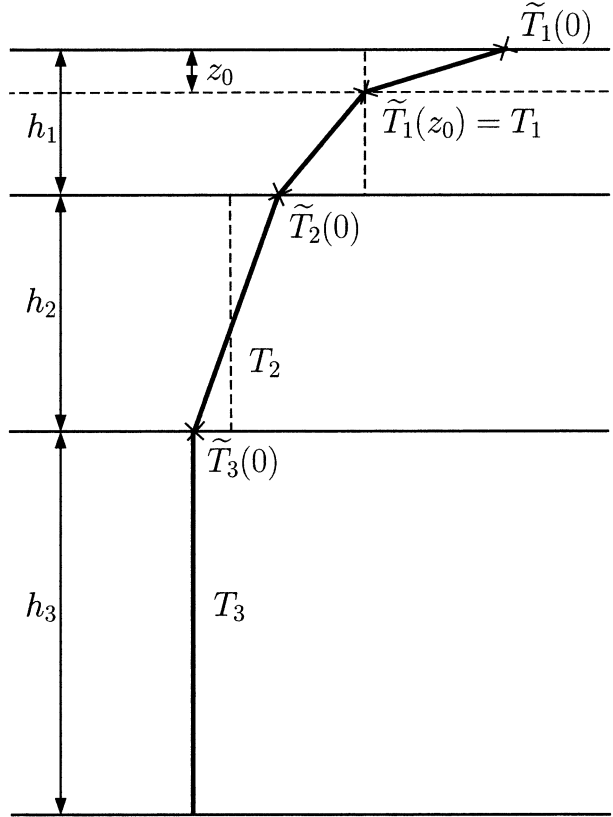


FIG. 2. Temperature profile used to specify the temperature at the base of the mixed layer (T_b) and stable MLD (h_s). Layer temperatures are denoted by $T_k (k = 1, 2, 3)$ and layer thicknesses h_k can move in time and space. For simplicity, only a three-layer structure is shown. Here, z_0 within layer 1 is the assigned depth for T_1 on the profile, and is chosen to make the layer 1 mean of \tilde{T} equal to T_1 . Note the profile is only valid below the mixed layer.

The sum specifies the interface temperature to be closer to that of the thinner layer. The nominal surface temperature $\tilde{T}_1(0)$ is the warmer of SST (T_m) and $T_1 + \Delta T_m$ [Eq. (17)], where ΔT_m is the temperature change across the mixed layer, and the layer 1 profile is split into two linear pieces chosen such that their layer average is T_1 . Note that the average of the profile over an interior layer thickness h_k is not T_k (as it should be for consistency). It would be possible to achieve this by using two linear pieces in such layers, as in layer 1, but the added computational cost was not judged worthwhile.

The mixed layer base temperature is

$$T_b = \tilde{T}(h_m), \quad (20)$$

and the stable MLD (h_s) is the shallowest depth at which

$$\tilde{T}(h_s) = T_m - \Delta T_m. \quad (21)$$

The overall surface to bottom temperature profile is

$$T(z) = \begin{cases} T_m - \frac{z}{h_m} \Delta T_m, & z \leq h_m, \\ \tilde{T}(z), & z > h_m, \end{cases} \quad (22)$$

with $T(0) = T_m$ and a discontinuity at h_m as required by bulk mixed layer theory.

The temperature change across the mixed layer, ΔT_m , is specified as a function of latitude based on the NRL mixed layer depth (NMLD) climatology (Kara et al. 2002b), and has values between 0.1°C at high latitudes and 1.5°C at low latitudes. The latitude dependence was determined using annual and monthly climatologies of surface ocean isothermal layer depths and MLDs (Kara et al. 2003) based on an optimal ocean layer depth definition (Kara et al. 2000a,b). Thus, $(T_m - \Delta T_m)$ is the temperature just above the base of the mixed layer, and T_b is the temperature just below the base of the mixed layer calculated from the NLOM temperature profile.

d. Turbulence model

The rate of mixed layer deepening or retreat, ω_m , is determined using a modified version of the KT model (Kraus and Turner 1967; Niiler and Kraus 1977). This involves solving the vertically integrated turbulent kinetic energy (TKE) equation for a stationary budget. The terms in the TKE budget (P) are parameterized using surface fluxes and variables integrated through the mixed layer as follows:

$$P = (m_3 - m_1)u_*^3 - h_m \left(\frac{n_c}{2} u_* b_* - \epsilon_b + m_5 \hat{f} u_*^2 \right), \quad (23)$$

$$u_*^2 = \frac{|\tau_a|}{\rho_0}, \quad (24)$$

$$u_* b_* = \frac{g\alpha(T_m)[Q_a - Q_p(h_m)]}{\rho_o C_{pw}}, \quad (25)$$

$$\epsilon_b = \begin{cases} m_6 u_* b_*, & u_* b_* < 0, \\ 0, & u_* b_* \geq 0, \end{cases} \quad (26)$$

$$\hat{f} = \max(|2\Omega \sin(\phi)|, f^+). \quad (27)$$

When shallowing (i.e., $P < 0$), mixing occurs toward the equilibrium depth as follows:

$$h_m^* = \frac{(m_3 - m_1)u_*^3}{\frac{n_c}{2} u_* b_* - \epsilon_b + m_5 \hat{f} u_*^2}, \quad (28)$$

$$\omega_m = \sigma_\omega [\max(h_m^*, h_m^+) - h_m]. \quad (29)$$

A relaxation timescale (σ_ω) is introduced to account for a delayed retreat of the mixed layer to the equilibrium depth. When deepening (i.e., $P > 0$), the available TKE is converted to potential energy as follows:

$$\omega_m = \frac{P}{g\alpha(T_m) \max(\Delta T_b, \Delta T_b^+) h_m}, \quad (30)$$

$$\Delta T_b = (T_m - \Delta T_m) - T_b. \quad (31)$$

If $[Q_a - Q_p(h_m)] < 0$ and $h_m < h_s$, entrainment toward the stable depth occurs at an entrainment rate of

$$\omega_m = \sigma_w (h_s - h_m). \quad (32)$$

A minimum value is imposed on the MLD [$h_m^+ = 10$ m; see Eq. (29)] because the formulation is not accurate for very shallow mixed layers. For example, velocity within the mixed layer is assumed to be \mathbf{v}_1 and a single exponential is used for attenuation of solar radiation with depth rather than multiple exponentials (e.g., Paulson and Simpson 1977; Zaneveld and Spinrad 1980). This minimum depth is also chosen to avoid skin effects at the ocean surface (Fairall et al. 1996), and is consistent with other OGCMs, which typically limit their minimum MLD to 10 m or more (e.g., Cherniawsky et al. 1990; Cherniawsky and Holloway 1991; Schopf and Loughe 1995).

Overall, ΔT_b [Eq. (31)] represents the temperature difference at the base of the mixed layer. It is a basic assumption of the bulk mixed layer approach that this temperature difference exists and is representable as a step function at the base of the mixed layer. Since ΔT_b is not guaranteed to be positive, an alternative minimum value ($\Delta T_b^+ = 0.2^\circ\text{C}$) is specified. A negative ΔT_b that could be representative of inversion layers (Sprintall and Roemmich 1999) still gives well-defined model equations and does not necessarily require drastic action since the mixed layer is only loosely coupled to the dynamical layers. It is an indication that the mixed layer is too shallow, and if there is surface cooling (indicating a possibly unstable mixed layer), the mixed layer is forced to deepen toward the depth at which it is stable with respect to T_b . The stable MLD [Eq. (21)] is based on the temperature profile extending through the dynamic layers. If there is surface heating, no special action is taken since heating and mixing already have a tendency to warm and shallow the mixed layer.

The KT model constants (m_1 , m_3 , m_5 , m_6 , and n_c) were originally determined from one-dimensional simulations of several idealized cases of wind-stirring, heating, and cooling, and they come with varying degrees of scientific backing. For example, m_5 is based on trying to get the correct neutral (zero surface heat flux) equilibrium mixed layer depth. Similarly, m_6 reduces the effectiveness of surface cooling. In other words, it allows for some dissipation when there is surface cooling and no wind. Its net effect is to reduce the depth of deep mixed layers. Since m_3 and m_1 are not independent in this version of KT, we set $m_3 = 7.5$ and $n_c = 1$, and tested various combinations of the other parameters over the ranges $1.25 \leq m_1 \leq 6.25$, $0.2 \leq (m_3 - m_1)/m_5 \leq 0.7$ and $0.0 \leq m_6 \leq 0.4$. Overall, $m_1 = 6.25$, $m_5 = 6.3$, and $m_6 = 0.3$ gave results that are close to the best in simulating SST over the entire global ocean (see section 3c).

3. Tuning of mixed layer parameters

All bulk mixed layer models contain free parameters with a range of plausible values. It is often possible to tune these parameters to give a realistic SST (and perhaps MLD) at a single point in the World Ocean over a wide range of atmospheric conditions (e.g., Martin 1985; Markus 1999; Nakamoto et al. 2001). However, this is only possible at the small number of locations with good quality multiyear observational datasets (e.g., Tabata and Weichselbaumer 1992). The optimal parameters are not necessarily the same at different locations, and the available locations are not necessarily representative of the global ocean. We are interested in finding a single set of parameters that provide a realistic SST from realistic atmospheric forcing over as much of the global ocean as possible. Our primary target is SST, rather than MLD, because it is better observed and more important to air–sea exchanges. On a global basis the most reliable source of truth is SST climatology. We therefore compare the monthly Comprehensive Ocean Atmosphere Data Set (COADS) SST (da Silva et al. 1994) climatology to monthly averages from the model forced by a climatological atmosphere (NLOM SST). It is not obvious that climatological atmospheric forcing should give rise to climatological SST. However, this approach allows relatively short model runs (e.g., 5 yr with the mixed layer) and greatly simplifies the parameter tuning process. Some care must be taken in configuring the climatological atmospheric forcing, but subsequent evaluation of the resulting optimal mixed layer parameters in multidecadal runs forced by 6-hourly fields from operational weather centers (not presented here) demonstrate the validity of the approach, at least for this particular mixed layer model.

a. Statistical measures

Tuning of the model parameters was performed using monthly means from the fifth year of the model run with an active mixed layer and comparing them with climatological data. Various statistical measures are considered together to measure the strength of the relationship between SST values predicted by the model and those from the climatology. We evaluate time series of monthly mean SST from January to December at each model grid point over the global ocean. Tuning of parameters is done by forming and examining zonally averaged statistical measures after each model simulation.

The statistical relationships used here (e.g., Murphy 1988; Laurent et al. 1998) between the 12 monthly mean COADS SST (X) and NLOM SST (Y) can be expressed as follows:

$$\text{ME} = \bar{Y} - \bar{X}, \quad (33)$$

$$\text{RMS} = \left[\frac{1}{n} \sum_{i=1}^n (Y_i - X_i)^2 \right]^{1/2}, \quad (34)$$

$$R = \frac{1}{n} \sum_{i=1}^n \frac{(X_i - \bar{X})(Y_i - \bar{Y})}{(\sigma_X \sigma_Y)}, \quad (35)$$

$$\text{SS} = R^2 - \underbrace{[R - (\sigma_Y/\sigma_X)]^2}_{B_C} - \underbrace{[(\bar{Y} - \bar{X})/\sigma_X]^2}_{B_{UC}}, \quad (36)$$

where $n = 12$, ME is the mean error, RMS is the root-mean-square difference, R is the correlation coefficient, SS is the skill score, and \bar{X} (\bar{Y}) and σ_X (σ_Y) are the mean and standard deviations of the COADS (NLOM) SST values, respectively. For the 12 monthly SST fields at each grid point over the global ocean, the R value between the NLOM and COADS SST must be at least ± 0.53 for it to be statistically different from a correlation coefficient of zero based on the Student's t test at the 95% confidence interval (Neter et al. 1988).

Because we need to examine more than the shape of the seasonal cycle using R , we also elected to use skill score, which includes conditional and unconditional biases (Murphy 1992). The nondimensional SS measures the accuracy¹ of SST simulations relative to COADS SST. The conditional bias is the bias in standard deviation of the NLOM SST [B_C , Eq. (36)]; while the unconditional bias reflects the mismatch between the mean NLOM and COADS SST [B_{UC} , Eq. (36)]. A simple definition for SS, based on RMS difference, is $\text{SS} = 1 - \text{RMS}^2/\sigma_X^2$ as given in Murphy and Daan (1985). Thus, in this study we use RMS difference as the basic measure of NLOM accuracy, and R^2 is equal to SS only when the conditional and unconditional biases are zero. The value of R^2 can be considered a measure of “potential” skill, that is, the skill that we can obtain by eliminating bias from the NLOM SST. Note the SS is 1.0 for perfect NLOM SSTs.

b. Model simulations

The model domain used for this study includes the global ocean between 72°S and 65°N, gridded to a resolution of 0.5° in latitude and 0.703125° in longitude. The lateral boundaries follow the 200-m isobath (with a few exceptions) and six active layers plus the mixed layer are used for the simulations reported here. The model time step is 36 min. All model simulations are performed using climatological monthly mean forcing fields. However, we add a high-frequency component to the climatological forcing because the mixed layer is known to be sensitive to variations in surface forcings on timescales of a day or less and because our goal is to perform simulations forced by high-frequency interannual atmospheric fields from operational weather centers.

For NLOM wind stress forcing (τ_{NLOM}), we use 6-

¹ Note here that accuracy refers to the match between NLOM and COADS SSTs, and skill refers to the NLOM SST accuracy relative to the COADS SST climatology.

hourly intramonthly anomalies from the European Centre for Medium-Range Weather Forecasts (ECMWF) operational weather forecast model (ECMWF 1995) in combination with the monthly mean wind stress climatology of Hellerman and Rosenstein (1983, hereafter HR), with interpolation between the monthly values as described below. For a reference year we chose to use the winds from September 1994 through September 1995, inclusive, because they represented a typical annual cycle of the ECMWF winds, and because the September winds in 1994 and 1995 most closely matched each other. In addition, winds in 1994 and 1995 were not strongly dominated by El Niño or La Niña. The 6-hourly September 1994 and September 1995 wind stresses are then blended to make a complete annual cycle, which we denote by τ_{ECMWF} . The ECMWF wind stresses are calculated from ECMWF 10-m winds using the bulk formulas of Kara et al. (2002b). To create the ECMWF wind stress anomalies (τ_A), we first form monthly averages from the September 1994 through September 1995 ECMWF wind stresses (τ_{ECMWF}), and then linearly interpolate them to the time intervals of the 6-hourly ECMWF winds to make a wind stress product (τ_I). The anomalies are then obtained by applying the difference $\tau_A = \tau_{\text{ECMWF}} - \tau_I$. For the climatological wind stress, we linearly interpolate the monthly mean to the time intervals of the 6-hourly ECMWF winds (τ_{HR}). By using these wind stresses (referred to as hybrid winds henceforth) we maintain compatibility with the spinup simulation without a mixed layer that was forced by the HR monthly wind stresses. Pure ECMWF wind products lead to unrealistic current patterns in some regions, and so a similar HR–ECMWF hybrid approach has been used for interannual winds in other ocean modeling studies (e.g., Metzger et al. 1992; Hurlburt et al. 1996; Metzger and Hurlburt 2001). Climatological monthly means of the thermal forcing are obtained from COADS. Thermal forcing includes shortwave (incoming solar) plus longwave radiation, air temperature at 10 m, and the air mixing ratio at 10 m. Scalar wind speed is obtained from the input wind stress and therefore has 6-hourly variability. Interannual NLOM simulations (not presented here) have confirmed that high-frequency wind variability has more impact on the mixed layer than high-frequency variability in other atmospheric forcing fields, at least when latent and sensible heat are calculated using both the ocean model mixed layer temperature (T_m) and the high-frequency wind speeds at each model time step.

All NLOM simulations presented in this paper are performed with no assimilation of oceanic data except for the relaxation of layer density to climatology. The model was spun up to statistical energy equilibrium without the mixed layer, that is, without heat flux forcing that uses the model SST, and then extended for 5 yr with surface heat fluxes determined from the atmospheric fields and SST provided by the model mixed layer. The monthly means of model SST are formed

from January through December of the last year of this simulation. Because all forcing is climatological these can then be compared with climatological monthly SST. The presence of the mixed layer has two major influences on NLOM simulations. First, it introduces much larger temporal and spatial variability in surface heat flux forcing in response to mesoscale dynamics, such as increased surface heating in coastal upwelling regions due to upwelling of colder water. Second, it induces greater temporal and spatial variability in the upper-ocean density as a consequence of the shallowing and deepening of the mixed layer. The impact of mixed layer penetration through the uppermost and underlying layers is most notable during periods of strong surface cooling as the layer densities are dramatically altered by the induced convection.

We first determine the best wind forcing to use for the model simulations using the statistical definitions. Traditionally, ocean modelers have used monthly wind stress climatologies constructed from marine surface observations such as Hellerman and Rosenstein (1983) to provide the wind forcing for climatological model simulations. To test the importance of using a high-frequency wind forcing in NLOM we performed two runs from the same initial state, one using monthly HR winds, a second with the 6-hourly ECMWF component added. The annual mean NLOM SST obtained using the monthly winds is much less accurate (see Fig. 3). The shape of the seasonal cycle (i.e., correlation coefficient) for the 12 monthly SST of NLOM versus COADS did not differ much over the global ocean between the two model simulations (Fig. 4). The global averages of these correlation coefficients are 0.90 and 0.92 for the monthly and hybrid wind forcing cases, respectively. On the other hand, the skill scores are quite different because they take the biases into account. The global averages of the skill scores are 0.41 and 0.74 for the monthly and hybrid wind forcing cases, respectively. Zonally averaged SS and R values shown in Fig. 5 indicate that the difference is largest at high latitudes and near the equator. It is possible that an alternative set of mixed layer parameters might perform as well with monthly winds as this set does with high-frequency winds. However, it is clear that a mixed layer model tuned with monthly winds cannot be optimal for interannual high-frequency forcing.

c. Choice of mixed layer parameters

The free parameters in this variant of the KT model are m_1 or $(m_3 - m_1)$, m_5 , and m_6 . A wide range of values have been reported for $(m_3 - m_1)$, but after extensive testing with $m_3 = 7.5$ and $1.25 \leq m_1 \leq 6.25$, we found that $m_1 = 6.25$ works best in this case. The neutral (zero surface heat flux) equilibrium mixed layer depth is $[(m_3 - m_1)/m_5](u_*^3/f)$. This implies that $(m_3 - m_1)/m_5$ should be between 0.2 and 0.7, that is, $1.8 \leq m_5 \leq 6.3$, with a larger m_5 leading to a shallower

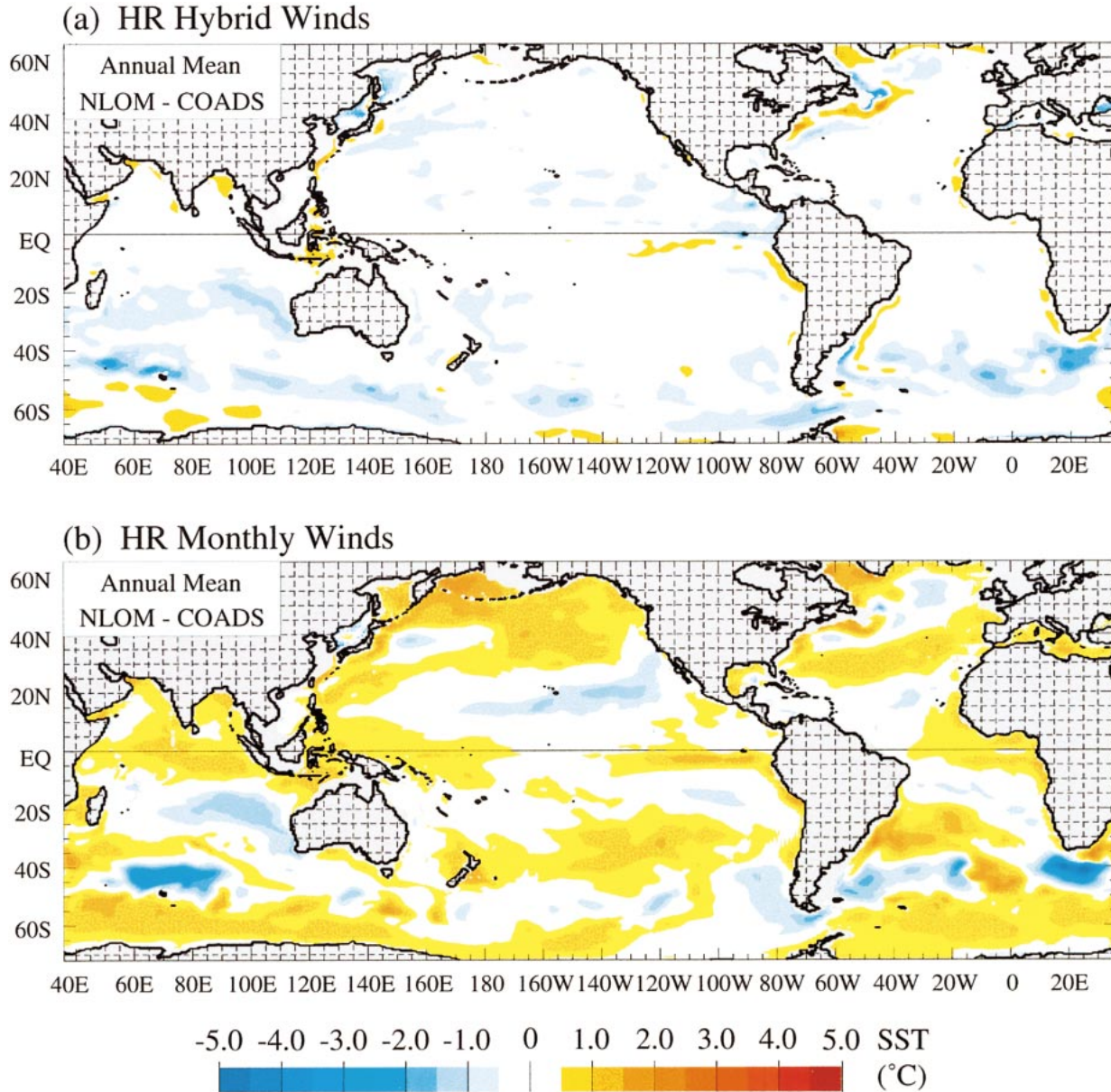


FIG. 3. Comparison of annual mean error in SST of NLOM with respect to COADS (NLOM-COADS). The NLOM with an embedded mixed layer is forced with (a) hybrid wind stress and (b) climatological HR monthly wind stress. The global RMS differences between the annual mean NLOM SST and annual mean COADS SST are 0.37° and 0.61°C for the hybrid wind stress case and climatological HR monthly wind stress case, respectively.

MLD. In cases of surface cooling, the stable equilibrium depth is approximately $2.5(m_3 - m_1)/(n_c/2 - m_6)L$, or $3.125L/(0.5 - m_6)$, where L is the Monin–Obukhov length. Based on the Deardorff (1972) parameterization for stable equilibrium depth $h_{eq} = (1/30L + f/0.35u_*^2)^{-1}$, we tried values of $m_6 \leq 0.4$ and found larger values of m_6 lead to a shallower MLD when there is surface cooling.

Figure 6 shows the sensitivity of the NLOM SST to the different KT parameter values for $m_1 = 6.25$. The

zonal averages, particularly of skill score, provide a robust indicator of the relative merits of each set of parameters. A significant improvement in one region is only rarely offset by a correspondingly large decline in another region. Typically, the improvement is for most latitudes or for one region with all others showing little change. We find the optimal KT parameters (which yield best agreement with COADS monthly SST) for NLOM are $m_1 = 6.25$, $m_3 = 7.5$, $m_5 = 6.3$, $m_6 = 0.3$, and $n_c = 1$. These parameter values are probably specific to this cou-

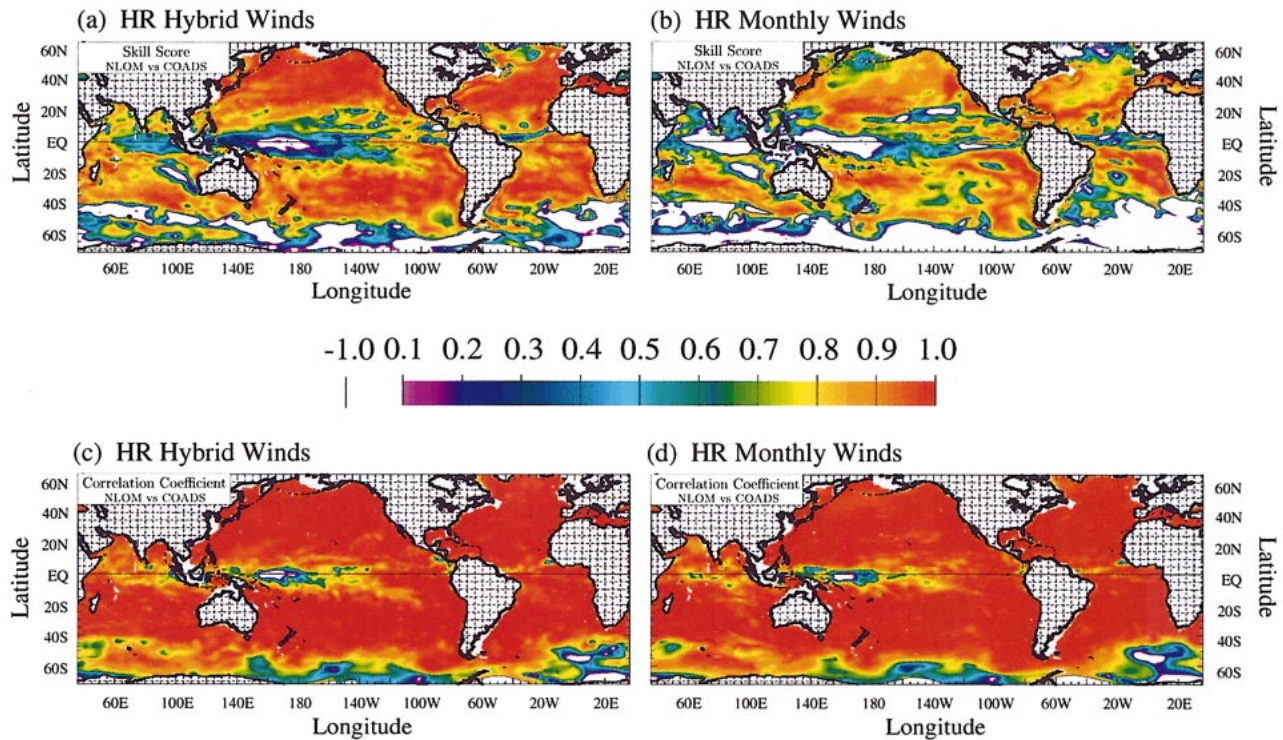


FIG. 4. Comparison of 12-monthly mean SST between COADS and NLOM using SS and R at each model grid point over the global ocean. (a) The SS values when NLOM is forced with hybrid wind stress, (b) SS values when NLOM is forced with monthly wind stress, (c) R values when NLOM is forced with hybrid wind stress, and (d) R values when NLOM is forced with monthly stress. Negative SS values indicate unskillful results. In these comparisons COADS is treated as “perfect.”

pled system, but the same methodology can be used to tune any mixed layer model with free parameters.

Other parameters affecting the mixed layer were also tuned by performing twin experiments with all other parameters held constant and comparing the resulting statistics. These included minimum mixed layer depth, minimum wind speed, and minimum temperature difference. Overall, the model simulations were not found to be very sensitive to these parameters in comparison to the KT parameters.

4. Conclusions

In this paper we have introduced the Naval Research Laboratory Layered Ocean Model (NLOM) with a newly developed bulk mixed layer submodel that carries prognostic equations for SST and MLD. This submodel is a variation of the Kraus–Turner (KT) mixed layer model and has been added as an option to the NLOM for simulating upper-ocean quantities. Coupling between the mixed layer submodel and the dynamical layers of the NLOM is achieved by explicitly distributing atmospheric forcing across the mixed layer (which can span multiple dynamic layers), and by making heat flux and thermal expansion dependent upon the mixed layer model’s SST. A major advantage of this approach is it

allows existing NLOM simulations spun up from rest without a mixed layer (requiring many hundreds of model years) to be used as the initial state for short runs with a mixed layer. This permits near-global multidecadal simulations with a mixed layer to be performed that are forced by realistic 6-hourly atmospheric forcing from operational weather center archives.

Considerable attention has been devoted to the construction of physically reasonable temperature profiles from the NLOM layer temperatures and tuning of KT parameters so that the embedded mixed layer submodel produces the best SST simulation. Care has also been taken to ensure that multiyear simulations meet the minimum requirement of no drift in yearly average SST over time. The combination of relaxing dynamical layer densities to climatology and having latent and sensible heat fluxes that are dependent upon the model SST is found to be sufficient to keep the SST on track without any explicit relaxation to the SST climatology.

The availability of free parameters with a range of plausible values makes it possible to tune the bulk KT mixed layer models to give realistic SST at a single location for a wide range of atmospheric conditions. Many papers have reported such choices for models that encompass regions up to basin scales. However, to our knowledge the study presented here is the first to attempt

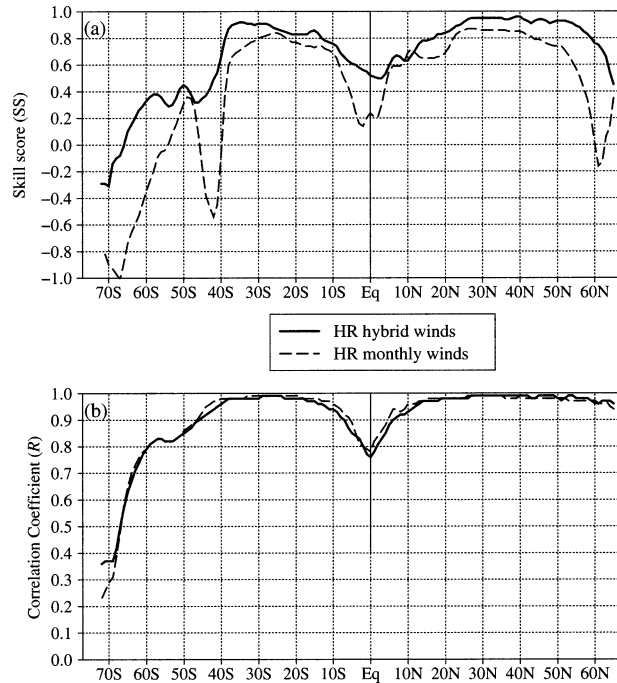


FIG. 5. Zonal averages of (a) nondimensional skill score and (b) correlation coefficient. Both measures are obtained using 12-monthly NLOM vs COADS SSTs when the NLOM is forced with HR and hybrid winds, separately. The zonal averaging is performed at each 1° latitude belt from 72°S to 65°N over the global ocean.

to tune a single set of KT parameters to produce an optimal SST over the global ocean with no relaxation/assimilation in the model to observed SST. It is also the first ocean model with low vertical resolution to demonstrate accurate SST globally. Using COADS SST as a baseline for comparison, we find that a careful choice of the KT parameters has to be made to produce monthly mean SST that is in excellent agreement over most of the global ocean. Although these actual parameter values are probably specific to the coupled system of the NLOM, they do provide some constraint on the range of values that can be considered “reasonable” in models encompassing more limited regions. This is especially true if one holds to the tenet that the KT parameters are space and time independent. We further note that high-frequency variability in atmospheric forcing must be used in this tuning process when developing a model for interannual studies. The methods and statistical metrics introduced here can also be used to tune any mixed layer model with free parameters.

Acknowledgments. We would like to extend our special thanks to E. J. Metzger of the Naval Research Laboratory (NRL) at Stennis Space Center for processing the atmospheric forcing fields used for the model simulations. We appreciate discussions with P. J. Martin and P. C. Gallacher of NRL during the preparation of this paper. Additional thanks go to D. Moore for his help in the

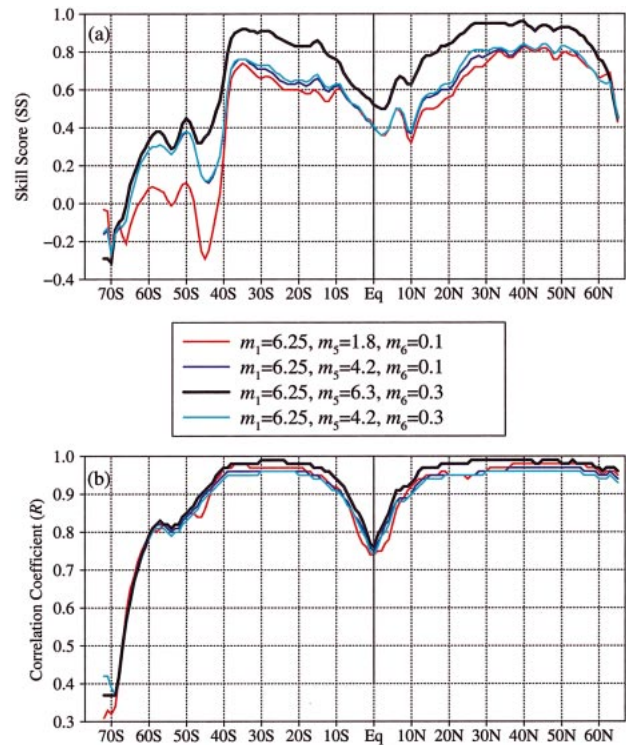


FIG. 6. An example of how the KT constants are tuned to obtain the best parameters for global ocean simulations. The nondimensional (a) skill score and (b) correlation coefficient are obtained using 12-monthly means of NLOM SST from the hybrid wind forced simulation with respect to the COADS SST. All other model parameters are kept constant in the simulations. Zonal averaging is as in Fig. 5.

model development. The ocean color data were obtained from the Goddard Distributed Active Archive Center under the auspices of the National Aeronautics and Space Administration. The authors would like to thank the SeaWiFS Project (Code 970.2) at the Goddard Space Flight Center, Greenbelt, Maryland, for the production and distribution of these data, respectively. Much appreciation is extended to the reviewers whose helpful comments improved the readability and quality of this paper. The numerical simulations were performed under the Department of Defense High Performance Computing Modernization Program, on an SGI Origin 2000 and a Cray T3E at the Naval Oceanographic Office, Stennis Space Center, Mississippi, and on a Cray T3E at the Arctic Region Supercomputer Center, Fairbanks, Alaska. This work was funded by the Office of Naval Research (ONR), and is a contribution of the Basin-Scale Prediction System project under Program Element 602435N, the Dynamics of Coupled Air–Ocean Models Study under Program Element 61153N, and the Thermodynamic and Topographic Forcing in Global Ocean Models project under Program Element 601153N. It was also funded through a National Partnership Program (NOPP) project, Monitoring the North Pacific for Improving Ocean Weather and Climate Forecasts. This NRL/JA contribution has been approved for public release.

APPENDIX A

Model Equations

The numerical ocean model used is a primitive equation layered formulation where the equations have been vertically integrated through each layer. The NLOM is a descendent of the model by Hurlburt and Thompson (1980) with significant enhancements by Wallcraft (1991), Wallcraft and Moore (1997), and Moore and Wallcraft (1998). It is available in both reduced gravity versions, where the lowest layer is infinitely deep and at rest, and finite-depth versions, which allow realistic bottom topography. Additionally, NLOM can be run in hydrodynamic mode (spatially and temporally constant density within each layer) or in thermodynamic mode (spatially and temporally varying density within each layer); that is, density is a prognostic variable. The model boundary conditions are kinematic and no slip.

The vertically integrated equations of motion used in the volume-conserving n -layer finite-depth thermodynamic model are given below, for layers $k = 1, 2, \dots, n$ with $k = 1$ for the top layer. When k is used to index the model interfaces, $k = 0$ at the surface and $k = n$ at the bottom. It is noted that the value of tunable parameters given below inside parentheses are for the $\frac{1}{2}^\circ$ global reference experiment. The NLOM equations are as follows:

$$\begin{aligned} & \frac{\partial U_k}{\partial t} + \frac{1}{a \cos \theta} \left[\frac{\partial(U_k u_k)}{\partial \phi} + \frac{\partial(V_k u_k \cos \theta)}{\partial \theta} - V_k(u_k \sin \theta + a\Omega \sin 2\theta) \right] \\ &= \max(0, -\omega_{k-1})u_{k-1} + \max(0, \omega_k)u_{k+1} - [\max(0, -\omega_k) + \max(0, \omega_{k-1})]u_k + \max(0, -C_M \omega_{k-1})(u_{k-1} - u_k) \\ &+ \max(0, C_M \omega_k)(u_{k+1} - u_k) - \frac{h_k}{a \cos \theta} \left\{ \sum_{j=1}^n \left[G_{kj} \frac{\partial(h_j - H_j)}{\partial \phi} + h_j \frac{\partial G_{kj}}{\partial \phi} \right] - \frac{g}{\rho_o} \left(\sum_{j=1}^{k-1} h_j + \frac{h_k}{2} \right) \frac{\partial \rho_k}{\partial \phi} \right\} \\ &+ \frac{(\tau_{\phi_{k-1}} - \tau_{\phi_k})}{\rho_o} + \frac{A_H}{a^2 \cos^2 \theta} \left[\frac{\partial(h_k e_{\phi \phi_k} \cos \theta)}{\partial \phi} + \frac{\partial(h_k e_{\phi \theta_k} \cos^2 \theta)}{\partial \theta} \right] \\ & \frac{\partial V_k}{\partial t} + \frac{1}{a \cos \theta} \left[\frac{\partial(U_k v_k)}{\partial \phi} + \frac{\partial(V_k v_k \cos \theta)}{\partial \theta} + U_k(u_k \sin \theta + a\Omega \sin 2\theta) \right] \\ &= \max(0, -\omega_{k-1})v_{k-1} + \max(0, \omega_k)v_{k+1} - [\max(0, -\omega_k) + \max(0, \omega_{k-1})]v_k + \max(0, -C_M \omega_{k-1})(v_{k-1} - v_k) \\ &+ \max(0, C_M \omega_k)(v_{k+1} - v_k) - \frac{h_k}{a} \left\{ \sum_{j=1}^n \left[G_{kj} \frac{\partial(h_j - H_j)}{\partial \theta} + h_j \frac{\partial G_{kj}}{\partial \theta} \right] - \frac{g}{\rho_o} \left(\sum_{j=1}^{k-1} h_j + \frac{h_k}{2} \right) \frac{\partial \rho_k}{\partial \theta} \right\} + \frac{(\tau_{\theta_{k-1}} - \tau_{\theta_k})}{\rho_o} \\ &+ \frac{A_H}{a^2 \cos^2 \theta} \left[\frac{\partial(h_k e_{\phi \theta_k} \cos \theta)}{\partial \phi} + \frac{\partial(h_k e_{\theta \theta_k} \cos^2 \theta)}{\partial \theta} \right], \\ & \frac{\partial h_k}{\partial t} + \nabla \cdot \mathbf{V}_k = \omega_k - \omega_{k-1} - \hat{K}_{H_k} \nabla^2 [\nabla^2 (h_k - H_k)] - \left(\frac{h_k}{\rho_k} \frac{\partial \hat{\rho}_k}{\partial t} - \frac{h_k}{\rho_k} \frac{\partial \overline{\hat{\rho}_k}}{\partial t} \right), \\ & \frac{\partial \rho_k}{\partial t} + \mathbf{v}_k \cdot \nabla \rho_k = \frac{\hat{\rho}_k}{\partial t} + \frac{\max(0, \omega_k)}{h_k} \max(0, \rho_{k+1} - \rho_k - \Delta \rho_k) - \frac{\max(0, -\omega_{k-1})}{h_k} \max(0, \rho_k - \rho_{k-1} - \Delta \rho_{k-1}), \quad \text{and} \\ & \frac{\partial \hat{\rho}_k}{\partial t} = \frac{H_o}{h_k} \sigma_\rho [\min(\rho_{k+1} - \Delta \rho_k, \hat{\rho}_k) - \rho_k] - \delta_{1k} \frac{Q}{c_{pw} \rho_o h_1} \frac{\partial \rho_1}{\partial T} + \frac{1}{h_k} [\nabla \cdot (h_k \nabla)] \left\{ K_H \rho_k - \frac{K_{H_k}}{h_k} [\nabla \cdot (h_k \nabla)] \rho_k \right\}, \end{aligned}$$

where

- A_H = coefficient of horizontal eddy viscosity ($1500 \text{ m}^2 \text{ s}^{-1}$),
- C_b = coefficient of bottom friction (2×10^{-3}),
- C_k = coefficient of interfacial friction (0),
- C_M = coefficient of additional interfacial friction associated with entrainment (1),
- $D(\phi, \theta)$ = total depth of the ocean at rest,

$$\nabla \cdot \mathbf{F} = \frac{1}{a \cos \theta} \frac{\partial F_\phi}{\partial \phi} + \frac{1}{a \cos \theta} \frac{\partial (F_\theta \cos \theta)}{\partial \theta},$$

$$G_{kj} = \begin{cases} g, & \text{for } j \geq k, \\ g - g(\rho_k - \rho_j)/\rho_o, & \text{for } j < k, \end{cases}$$

H_k = k th-layer thickness at rest in m (65, 175, 260, 400, 600, bottom),

$$H_n = D(\phi, \theta) - \sum_{j=1}^{n-1} H_j,$$

H_o = constant reference layer thickness for density relaxation (100 m),

K_H = coefficient of horizontal density diffusivity ($300 \text{ m}^2 \text{ s}^{-1}$),

K_{H_4} = coefficient of biharmonic horizontal density diffusivity ($-300 \times 10^{11} \text{ m}^4 \text{ s}^{-1}$),

\tilde{K}_{H_4} = coefficient of biharmonic horizontal layer thickness diffusivity ($-300 \times 10^{11} \text{ m}^4 \text{ s}^{-1}$),

\bar{Q} = total surface heat flux from the mixed layer model,

\hat{T}_1 = layer 1 temperature climatology,

$$\mathbf{V}_k = h_k \mathbf{v}_k = \mathbf{e}_\phi U_k + \mathbf{e}_\theta V_k,$$

$W_k(\phi, \theta)$ = k th interface weighting factor for global vertical mixing designed to conserve mass within a layer in compensation for explicit vertical mixing due to $h_k < h_k^+$,

$\overline{X(\phi, \theta)}$ = domain wide area average of X ,

a = radius of the earth (6371 km),

c_{pw} = specific heat of seawater ($3993 \text{ J kg}^{-1} \text{ K}^{-1}$),

\mathbf{e}_k = angular deformation tensor,

$$e_{\phi\phi_k} = \frac{\partial}{\partial \phi} \left(\frac{u_k}{\cos \theta} \right) - \cos \theta \frac{\partial}{\partial \theta} \left(\frac{v_k}{\cos \theta} \right) = -e_{\theta\theta_k},$$

$$e_{\phi\theta_k} = \frac{\partial}{\partial \phi} \left(\frac{v_k}{\cos \theta} \right) + \cos \theta \frac{\partial}{\partial \theta} \left(\frac{u_k}{\cos \theta} \right) = e_{\theta\phi_k},$$

g = acceleration due to gravity (9.81 m s^{-2}),

h_k = k th-layer thickness,

h_k^+ = k th-layer thickness at which entrainment starts [50 m ($k = 1$), 40 m ($k = 2-6$)],

h_k^- = k th-layer thickness at which detrainment starts; not used by setting to a large value,

$\max(A, B)$ = use the maximum value of the arguments A and B ,

t = time,

\mathbf{v}_k = k th-layer velocity = $\mathbf{e}_\phi u_k + \mathbf{e}_\theta v_k$,

$$\nabla \Phi = \frac{1}{a \cos \theta} \frac{\partial \Phi}{\partial \phi} \mathbf{e}_\phi + \frac{1}{a} \frac{\partial \Phi}{\partial \theta} \mathbf{e}_\theta,$$

$$\nabla^2 \Phi = \frac{1}{a^2 \cos^2 \theta} \frac{\partial^2 \Phi}{\partial \phi^2} + \frac{1}{a^2 \cos \theta} \frac{\partial}{\partial \theta} \left(\frac{\partial \Phi}{\partial \theta} \cos \theta \right),$$

Ω = the earth's angular rotation rate ($7.292205 \times 10^{-5} \text{ s}^{-1}$),

ϕ = longitude,

θ = latitude,

ρ_k = k th-layer density,

$\hat{\rho}_k(\phi, \theta)$ = k th-layer density climatology,

$\Delta \rho_k$ = k th interface minimum density shear,

ρ_o = reference density (1000 kg m^{-3}),

$$\frac{\partial \rho_1}{\partial T} = 5.3 \times 10^{-5} + 1.2 \times 10^{-5} T - 9.7 \times 10^{-8} T^2,$$

σ_ρ = reference coefficient of density climatology relaxation,

$$\boldsymbol{\tau}_k = \begin{cases} \boldsymbol{\tau}_\omega, & \text{for } k = 0 \\ C_k \rho_o |\mathbf{v}_k - \mathbf{v}_{k-1}| (\mathbf{v}_k - \mathbf{v}_{k+1}), & \text{for } k = 1, 2, \dots, n-1 \\ C_b \rho_o |\mathbf{v}_n| \mathbf{v}_n, & \text{for } k = n, \end{cases}$$

$\boldsymbol{\tau}_\omega$ = wind stress,

$$\omega_k = \begin{cases} 0, & \text{for } k = 0, n \\ \omega_k^+ - \omega_k^- - W_k \hat{\omega}_k, & \text{for } k = 1, 2, \dots, n-1, \end{cases}$$

$$\begin{aligned}\Omega_k^+ &= \tilde{\omega}_k [\max(0, h_k^+ - h_k)/h_k^+]^2, \\ \omega_k^- &= \tilde{\omega}_k [\max(0, h_k - h_k^-)/h_k^-]^2, \\ \hat{\omega}_k &= (\omega_k^+ - \omega_k^-)/\bar{W}_k, \text{ and} \\ \tilde{\omega}_k &= k\text{th interface reference entrainment velocity (0.1 m s}^{-1}\text{)}.\end{aligned}$$

APPENDIX B

Symbol Definitions

Listed here for convenience of reference are the various symbols used within the text along with a brief description. Note that tunable parameters provided below are for the $\frac{1}{2}^\circ$ global reference experiment.

Symbol description

C_{pa}	Specific heat of air (1004.5 J kg ⁻¹ K ⁻¹)
C_{pw}	Specific heat of water (3993 J kg ⁻¹ K ⁻¹)
f^+	Coriolis parameter at 5° latitude (2.5×10^{-5} s ⁻¹)
g	Gravitational acceleration (9.81 m s ⁻²)
h_k	k th-layer thickness (m)
h_m	Mixed layer depth (m)
h_m^+	Minimum mixed layer depth (10 m)
h_m^*	Mixed layer equilibrium depth (m)
h_p	Radiation absorption length scale (m)
h_s	Stable mixed layer depth (m)
k_{PAR}	Diffusive attenuation coefficient (m ⁻¹)
K_H	Coefficient of horizontal temperature diffusivity (0 m ² s ⁻¹)
m_i	Turbulent kinetic energy (TKE) constants ($m_1 = 6.25$, $m_3 = 7.5$, $m_5 = 6.3$, $m_6 = 0.3$)
n_c	TKE constant ($n_c = 1$)
P	Net rate of generation of available TKE (m ³ s ⁻³)
Q_a	Net heat flux at the sea surface (W m ⁻²)
Q_{IR}	Infrared radiation (W m ⁻²)
Q_L	Latent heat flux (W m ⁻²)
Q_{LW}	Net longwave radiation at the sea surface (W m ⁻²)
Q_p	Penetrating solar radiation (W m ⁻²)
$Q_p(z)$	Penetrating radiation at depth z (W m ⁻²)
Q_s	Sensible heat flux (W m ⁻²)
Q_{SOL}	Solar irradiance at the sea surface (W m ⁻²)
$Q(z)$	Net heat flux at depth z (W m ⁻²)
t	Time (s)
$\tilde{T}(z)$	Continuous temperature profile
$\tilde{T}(h_s)$	Temperature at the stable depth (°C)
T_b	Temperature just below the mixed layer (°C)
T_k	k th-layer temperature (°C)
\hat{T}_k	Observed temperature climatology for layer k (°C)
$\tilde{T}_k(z)$	Continuous temperature profile in layer k (°C)
T_m	Sea surface temperature (°C)
u_*	Friction velocity (m s ⁻¹)
$u_* b_*$	Buoyancy (m ² s ⁻³)
v_1	Layer 1 velocity (m s ⁻¹)
$\alpha(T)$	Coefficient of thermal expansion of seawater (°C ⁻¹)

ΔT_b	Temperature difference at the base of the mixed layer (°C)
ΔT_b^+	Minimum temperature difference (0.2°C)
ΔT_m	Temperature change across the mixed layer (°C)
ϵ_b	Rate of background dissipation (m ² s ⁻³)
λ_p	Photosynthetically available radiation (PAR) fraction of the solar irradiance at the sea surface (0.49)
ω_m	Entrainment velocity (m s ⁻¹)
Ω	Rotation rate of the earth (7.292×10^{-5} s ⁻¹)
ρ_a	Density of air near the sea interface (kg m ⁻³)
ρ_k	k th-layer density (kg m ⁻³)
$\hat{\rho}_k$	Observed density climatology for layer k (kg m ⁻³)
$\tilde{\rho}_k$	Model density climatology for layer k (kg m ⁻³)
ρ_0	Reference density (1000 kg m ⁻³)
σ_ω^{-1}	Mixed layer depth (MLD) relaxation e -folding time (s)

REFERENCES

- Carpenter, R. L., Jr., K. K. Drogemeier, P. R. Woodward, and C. E. Hane, 1990: Application of the piecewise parabolic method to meteorological modeling. *Mon. Wea. Rev.*, **118**, 586–612.
- Cherniawsky, J. Y., and G. Holloway, 1991: An upper-ocean general circulation model for the North Pacific: Preliminary experiments. *Atmos.–Ocean*, **29**, 737–784.
- , C. W. Yuen, C. A. Lin, and L. A. Mysak, 1990: Numerical experiments with a wind- and buoyancy-driven two-and-half-layer upper ocean model. *J. Geophys. Res.*, **95**, 16 149–16 167.
- da Silva, A. M., C. C. Young, and S. Levitus, 1994: *Algorithms and Procedures*. Vol. 1, *Atlas of Surface Marine Data*, NOAA Atlas NESDIS **6**, 83 pp.
- Deardorff, J. W., 1972: Parameterization of the planetary boundary layer for use in general circulation models. *Mon. Wea. Rev.*, **100**, 93–106.
- ECMWF, 1995: User guide to ECMWF products. ECMWF Meteorological Bulletin M3.2, 71 pp. [Available from ECMWF, Shinfield Park, Reading RG2 9AX, United Kingdom.]
- Fairall, C. W., E. F. Bradley, J. S. Godfrey, G. A. Wick, J. B. Edson, and G. S. Young, 1996: Cool skin and warm layer effects on sea surface temperature. *J. Geophys. Res.*, **101**, 1295–1308.
- Garwood, R. W., 1977: An oceanic mixed layer model capable of simulating cyclic states. *J. Phys. Oceanogr.*, **7**, 455–468.
- Gent, P. R., and M. A. Cane, 1989: A reduced gravity, primitive equation model of the upper equatorial ocean. *J. Comput. Phys.*, **81**, 444–480.
- Gill, A. E., 1982: *Atmosphere–Ocean Dynamics*. International Geophysical Series, Vol. 30, Academic Press, 662 pp.
- Hellerman, S., and M. Rosenstein, 1983: Normal monthly wind stress over the world ocean with error estimates. *J. Phys. Oceanogr.*, **13**, 1093–1104.
- Hu, D., and Y. Chao, 1999: A global isopycnal OGCM: Validations using observed upper-ocean variabilities during 1992–93. *Mon. Wea. Rev.*, **127**, 706–725.
- Hurlburt, H. E., and J. D. Thompson, 1980: A numerical study of

- Loop Current intrusions and eddy shedding. *J. Phys. Oceanogr.*, **10**, 1611–1651.
- , A. J. Wallcraft, W. J. Schmitz Jr., P. J. Hogan, and E. J. Metzger, 1996: Dynamics of the Kuroshio/Oyashio current system using eddy-resolving models of the North Pacific Ocean. *J. Geophys. Res.*, **101**, 941–976.
- Jacobs, G. A., H. E. Hurlburt, J. C. Kindle, E. J. Metzger, J. L. Mitchell, W. J. Teague, and A. J. Wallcraft, 1994: Decade-scale trans-Pacific propagation and warming effects of an El Niño anomaly. *Nature*, **370**, 360–363.
- Kantha, L. H., and C. A. Clayson, 1994: An improved mixed layer model for geophysical applications. *J. Geophys. Res.*, **99**, 25 235–25 266.
- Kara, A. B., P. A. Rochford, and H. E. Hurlburt, 2000a: An optimal definition for ocean mixed layer depth. *J. Geophys. Res.*, **105**, 16 803–16 821.
- , —, and —, 2000b: Mixed layer depth variability and barrier layer formation over the North Pacific Ocean. *J. Geophys. Res.*, **105**, 16 783–16 801.
- , —, and —, 2002a: Air–sea flux estimates and the 1997–1998 ENSO event. *Bound.-Layer Meteor.*, **103**, 439–458.
- , —, and —, 2002b: Naval Research Laboratory Mixed Layer Depth (NMLD) climatologies. NRL Rep. NRL/FR/7330/02/9995, 26 pp. [Available from Naval Research Laboratory, Code 7323, Stennis Space Center, MS 39529-5004.]
- , —, and —, 2003: Mixed layer depth variability over the global ocean. *J. Geophys. Res.*, **108**, doi:10.1029/2000JC000736.
- Kraus, E. B., and J. S. Turner, 1967: A one-dimensional model of the seasonal thermocline: II. The general theory and its consequences. *Tellus*, **19**, 98–106.
- Large, W. G., J. C. McWilliams, and S. C. Doney, 1994: Oceanic vertical mixing: A review and a model with a nonlocal boundary layer parameterization. *Rev. Geophys.*, **32**, 363–403.
- Laurent, H., I. Jobard, and A. Toma, 1998: Validation of satellite and ground-based estimates of precipitation over the Sahel. *Atmos. Res.*, **47–48**, 651–670.
- Levitus, S., and T. P. Boyer, 1994: *Temperature*. Vol. 4, *World Ocean Atlas 1994*, NOAA Atlas NESDIS 4, 117 pp.
- Lin, S.-J., W. C. Chao, Y. C. Sud, and G. K. Walker, 1994: A class of the van Leer-type transport schemes and its application to the moisture transport in a general circulation model. *Mon. Wea. Rev.*, **122**, 1575–1593.
- Markus, T., 1999: Results from an ECMWF-SSM/I forced mixed layer model of the Southern Ocean. *J. Geophys. Res.*, **104**, 15 603–15 620.
- Martin, P., 1985: Simulation of the mixed layer at OWS November and Papa with several models. *J. Geophys. Res.*, **90**, 903–916.
- McClain, C. R., M. L. Cleave, G. C. Feldman, W. W. Gregg, S. B. Hooker, and N. Kuring, 1998: Science quality SeaWiFS data for global biosphere research. *Sea Technol.*, **39**, 10–16.
- McCreary, J. P., P. K. Kundu, and R. L. Molinari, 1993: A numerical investigation of dynamics, thermodynamics, and mixed layer processes in the Indian Ocean. *Progress in Oceanography*, Vol. 31, Pergamon, 181–244.
- Mellor, G. L., and T. Yamada, 1982: Development of a turbulence closure model for geophysical fluid problems. *Rev. Geophys. Space Phys.*, **20**, 851–875.
- Metzger, E. J., and H. E. Hurlburt, 2001: The nondeterministic nature of Kuroshio penetration and eddy shedding in the South China Sea. *J. Phys. Oceanogr.*, **31**, 1712–1732.
- , —, J. C. Kindle, Z. Sirkes, and J. M. Pringle, 1992: Hindcasting of wind-driven anomalies using a reduced-gravity global ocean model. *Mar. Technol. Soc. J.*, **26**, 23–32.
- Moore, D. R., and A. J. Wallcraft, 1998: Formulation of the NRL Layered Ocean Model in spherical coordinates. NRL Rep. NRL/CR/7323-96-0005, 24 pp. [Available from Naval Research Laboratory, Code 7323, Stennis Space Center, MS 39529-5004.]
- Murphy, A. H., 1988: Skill scores based on the mean square error and their relationships to the correlation coefficient. *Mon. Wea. Rev.*, **116**, 2417–2424.
- , 1992: Climatology, persistence, and their linear combination as standards of reference in skill scores. *Wea. Forecasting*, **7**, 692–698.
- , and H. Daan, 1985: Forecast evaluation. *Probability, Statistics, and Decision Making in the Atmospheric Sciences*, A. H. Murphy and R. W. Katz, Eds., Westview Press, 379–437.
- Murtugudde, R., M. Cane, and V. Prasad, 1995: A reduced-gravity, primitive equation, isopycnal ocean GCM: Formulation and simulations. *Mon. Wea. Rev.*, **123**, 2864–2887.
- Nakamoto, S., S. P. Kumar, J. M. Oberhuber, J. Ishizaka, K. Muneyama, and R. Frouin, 2001: Response of the equatorial Pacific to chlorophyll pigment in a mixed layer isopycnal ocean general circulation model. *Geophys. Res. Lett.*, **28**, 2021–2024.
- Neter, J., W. Wasserman, and G. A. Whitmore, 1988: *Applied Statistics*. Allyn and Bacon, 1006 pp.
- Niiler, P. P., and E. B. Kraus, 1977: One-dimensional models of the upper ocean. *Modeling and Prediction of the Upper Layers of the Ocean*, E. B. Kraus, Ed., Pergamon Press, 143–172.
- Paulson, C. A., and J. J. Simpson, 1977: Irradiance measurements in the upper ocean. *J. Phys. Oceanogr.*, **7**, 952–956.
- Price, J. F., R. A. Weller, and R. Pinkel, 1986: Diurnal cycling: Observations and models of the upper ocean response to diurnal heating, cooling, and wind mixing. *J. Geophys. Res.*, **91**, 8411–8427.
- Rhodes, R. C., H. E. Hurlburt, A. J. Wallcraft, C. N. Barron, P. J. Martin, E. J. Metzger, J. F. Shriver, and D. S. Ko, 2002: Navy real-time global modeling systems. *Oceanography*, **15** (1), 29–43.
- Rochford, P. A., J. C. Kindle, P. C. Gallacher, and R. A. Weller, 2000: Sensitivity of Arabian Sea mixed layer to 1994–1995 operational wind products. *J. Geophys. Res.*, **105**, 14 141–14 162.
- , A. B. Kara, A. J. Wallcraft, and R. A. Arnone, 2001: Importance of solar subsurface heating in ocean general circulation models. *J. Geophys. Res.*, **106**, 30 923–30 938.
- Rodi, W., 1987: Examples of calculation methods for flow and mixing in stratified fluids. *J. Geophys. Res.*, **92**, 5305–5328.
- Schopf, P. S., and A. Loughe, 1995: A reduced-gravity isopycnal ocean model: Hindcasts of El Niño. *Mon. Wea. Rev.*, **123**, 2839–2863.
- Simpson, J. J., and T. D. Dickey, 1981: Alternative parameterizations of downward solar irradiance and their dynamical significance. *J. Phys. Oceanogr.*, **11**, 876–882.
- Smedstad, O. M., H. E. Hurlburt, E. J. Metzger, R. C. Rhodes, J. F. Shriver, A. J. Wallcraft, and A. B. Kara, 2003: An operational eddy-resolving 1/16° global ocean nowcast forecast system. *J. Mar. Syst.*, **40–41**, 341–361.
- Sprintall, J., and D. Roemmich, 1999: Characterizing the structure of the surface layer in the Pacific Ocean. *J. Geophys. Res.*, **104**, 23 297–23 311.
- Stull, R. B., 1988: *An Introduction to Boundary Layer Meteorology*. Kluwer, 666 pp.
- Tabata, S., and W. E. Weichselbaumer, 1992: An update of the statistics of oceanographic data based on hydrographic/CTD casts made at stations 1 through 6 along line P during January 1959 through September 1990. Canadian Data Rep. Hydrography and Ocean Sciences No. 108, 317 pp.
- Wallcraft, A. J., 1991: The Navy Layered Ocean Model users guide. NOARL Tech. Rep., 35, 21 pp. [Available from Naval Research Laboratory, Code 7323, Stennis Space Center, MS 39529-5004.]
- , and D. R. Moore, 1997: The NRL Layered Ocean Model. *Parallel Comput.*, **23**, 2227–2242.
- Warn-Varnas, A. C., and S. A. Piacsek, 1979: An investigation of the importance of third-order correlations and choice of length scale in mixed layer modeling. *Geophys. Astrophys. Fluid Dyn.*, **13**, 225–243.
- Yuen, C. W., J. Y. Cherniawsky, C. A. Lin, and L. A. Mysak, 1992: An upper ocean general circulation model for climate studies: Global simulation with seasonal cycle. *Climate Dyn.*, **7**, 1–18.
- Zaneveld, J. R., and R. W. Spinrad, 1980: An arctangent model of irradiance in the sea. *J. Geophys. Res.*, **85**, 4919–4922.